Influence of atmosphere kind on temperature programmed decomposition of noble metal chlorides

Wojciech K. Jóźwiak, Tomasz P. Maniecki *

*Institute of General and Ecological Chemistry, Technical University of Łódź,
Żeromskiego 116, 90-924 Łódź, Poland*

Abstract

The hydrated chlorides of noble metals located in the 8–10 groups of Periodic System were used in this work: Ru, Rh, Pd, Ir and Pt. The common mechanism of chloride compounds decomposition in oxidative, inert and reductive atmospheres was postulated and mutual similarities and differences were discussed. These compounds play a significant role in heterogeneous catalysis, as starting materials for metal/oxide catalysts, and also in analytical chemistry and industry.
© 2005 Elsevier B.V. All rights reserved.

1. Introduction

Thermal stability of the 8–10 group noble metal chlorides was the subject of many papers in the last 50 years [1,2]. Most papers refer only to individual compounds, narrow range of temperature—usually lower than 500 °C and air atmosphere. However, there is still a shortage of comparative study describing the thermal behavior of metal chlorides in the wide temperature range (up to 1500 °C) and in different atmospheres: neutral—helium or argon, oxidative—air or oxygen and reductive—hydrogen or carbon monoxide.

Chlorides play a significant role in heterogeneous catalysis, as starting materials for metal/oxide catalysts, also in analytical chemistry and industry. Knowledge of physicochemical properties of noble metal chlorides is closely related to many aspects of applied and pure catalysis. Noble metal chlorides and nitrates are widely used as precursors for active metal phase highly dispersed on oxide supports. Also, physico-chemical properties of metal/oxide catalysts are strongly influenced by the presence of chlorine ions involved in metal–oxide interactions [3]. Metal chlorides,

cheaper than metal nitrates, play an important role in many stages of catalyst preparation: kind and conditions of procedure, activation, reduction and finally, catalytic activity [4]. Chlorine "free" metal/oxide support catalysts usually behave differently from those containing chlorine ions. In the case of alumina, silica and titania supported metal catalysts, even the high temperature range of treatment (800–1000 °C) does not assure chlorine free catalyst surface. Decomposition of chlorine-organic compounds, oxy-dechlorination and hydro-dechlorination (HCFC, dioxins, PCV and others) are carried out on noble metal/support catalysts [5–10]. Also the effect of chlorine on catalytic activity in oxidation of methane [11], reduction of unsaturated aldehydes [12] and WGS reaction [13].

Relatively little is known about the mechanism of thermal decomposition of noble metal chlorides. Shaplygin and Lazarev have investigated the behavior of Ru, Rh and Pd chlorides in air atmosphere but the intermediate products of decomposition were not reported [1]. Peczkowski and Vorobiev [6] published some details referring to the mechanistic approach to iron II and III chlorides decomposition in air. Papers by Livingstone [7] and Ginzburg [8] devoted to analytical chemistry of noble metals do not contain information about the influence of temperature and atmosphere on metal chlorides decomposition. This work

* Corresponding author. Tel.: +48 426313125; fax: +48 426313127.
  E-mail addresses: wjozwiak@mail.p.lodz.pl (W.K. Jóźwiak),
tmanieck@mail.p.lodz.pl (T.P. Maniecki).

Table 1
Hydrated chlorides of noble metals from 8 to 10 groups of Periodic System

No.	Compounds	Formula	Producer
1	Ruthenium III chloride	$RuCl_3 \cdot nH_2O$	Koch–Light Laboratory
2	Rhodium III chloride	$RhCl_3 \cdot 3H_2O$	Koch–Light Laboratory
3	Palladium II chloride	$PdCl_2$	POCH–Gliwice
4	Iridium III chloride	$IrCl_3 \cdot 3H_2O$	Merck
5	Platinum IV chloride	$PtCl_4 \cdot 5H_2O$	Aldrich

is devoted to the comparative study of thermal behavior of the noble metal hydrated chlorides: Ru, Rh, Pd, Ir and Pt in the wide temperature range, up to 1500 °C and in different atmospheres: oxidative, neutral and reductive.

2. Experimental

2.1. Materials

The commercial compounds—noble metal chlorides, used in this work, are presented in Table 1 containing name, chemical formula and producer.

2.2. Methods

Thermo-gravimetric TG method, equipped with differential thermal analysis DTA device SETSYS-16/18 (Setaram) and combined in line with quadrupole mass spectrometer MS Thermostar (Balzers) were used for temperature programmed decomposition of noble metal chlorides in three different gaseous atmospheres: oxidative 2% O_2–98% Ar, neutral Ar 5.0 and reductive 2% H_2–98% Ar. The TG–DTA–MS measurements were carried out applying sample weight about 20 mg, linear heating rate of 10 °C/min, temperature range from 25 up to 1500 °C. Most samples were used without any preliminary treatment with the exception of ruthenium III chloride—$RuCl_3 \cdot nH_2O$ pretreated in vacuum at 50 °C. The order of TG–DTA–MS measurements is the same as the location of noble metals in the 8–10 groups of Periodic System i.e. Ru, Rh, Pd, Ir and Pt, respectively.

3. Results

3.1. Ruthenium III chloride—$RuCl_3 \cdot nH_2O$

The decomposition of ruthenium III chloride $RuCl_3 \cdot nH_2O$ in oxidative atmosphere 2% O_2–98% Ar is presented in Fig. 1. Curves TG, DTG and DTA are located in upper part (a), whereas MS profiles ($m/z = 18$—H_2O, $m/z = 32$—O_2, $m/z = 36$—HCl, $m/z = 70$—Cl_2) are located in lower part (b) of this figure. Sample decomposition starts at about 50 °C and the changes of TG and DTG curves are accompanied by one strong and two much smaller endotermic DTA effects. The evolution of water represented by: MS profile ($m/z = 18$), TG, DTG and DTA curves shows that sample dehydra-
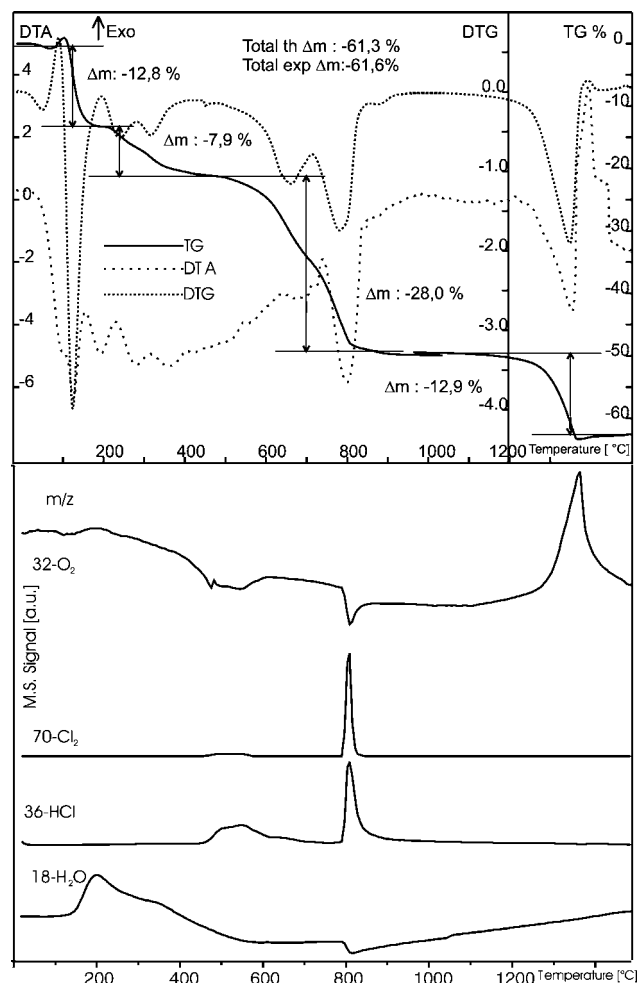

Fig. 1. Thermal decomposition of $RuCl \cdot nH_2O$ in oxidative atmosphere (2% O_2–98% Ar).

tion is at least a three-step process ending at about 400 °C and comprising about 21% of mass sample decrease. In the range of temperature 400–700 °C the first stage of sample dechlorination–oxidation takes place manifesting the evolution of HCl ($m/z = 36$) and the consumption of O_2 ($m/z = 32$). The second stage of dechlorination occurs in temperature range 700–850 °C and is accompanied by rather strong DTA endothermic effect and narrow but comparable evolution of HCl ($m/z = 36$) and Cl_2 ($m/z = 70$). Oxygen and water uptakes can be observed O_2 ($m/z = 32$) and H_2O ($m/z = 18$), respectively. The weight decrease in this region was about 28%. Above 1000 °C sample de-oxidation takes place and this process is illustrated by TG, DTG changes (Δm about 12.9%) and a strong endothermic DTA effect accompanied by MS oxygen evolution ($m/z = 32$). These results confirm $RuCl_3 \rightarrow RuO_2$ transformation with the increase of ruthenium oxidation number Ru(III) → Ru(IV) occurring during dechlorination-oxidation stage. The evolution of oxygen represents the last stage of sample decomposition above 1000 °C $RuO_2 \rightarrow Ru^0 + O_2$. The total change of sample mass was about 61.6%. The following sequence of successive events
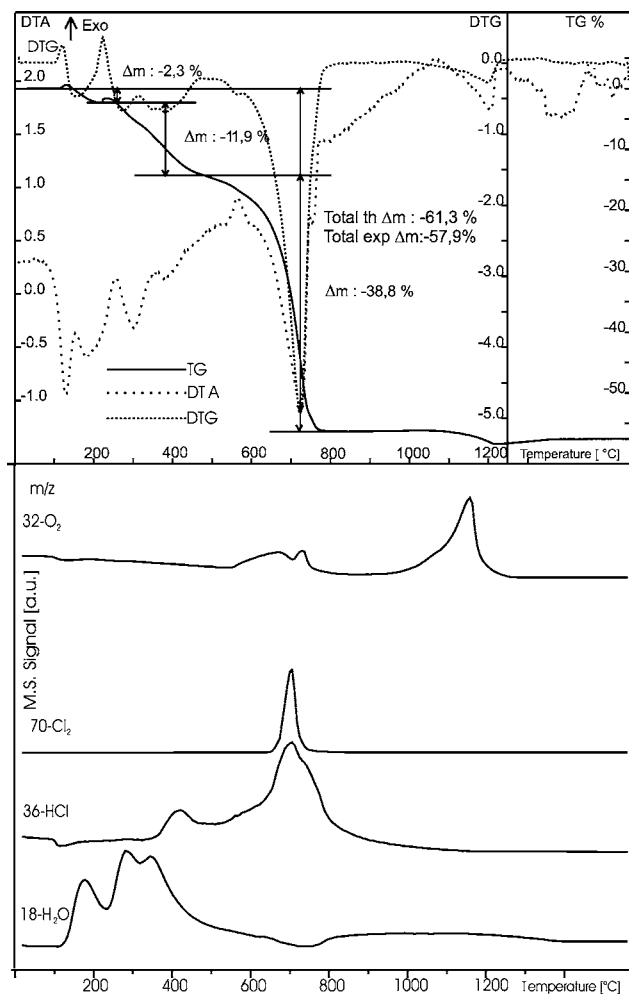
Fig. 2. Thermal decomposition of $RuCl_3 \cdot nH_2O$ in inert atmosphere (Ar).

Fig. 3. Thermal decomposition of $RuCl_3 \cdot nH_2O$ in reductive atmosphere (2% H_2–98% Ar).

can be anticipated: dehydration, dechlorination plus oxidation and finally thermal dissociation of ruthenium oxide leading to metal phase.

The decomposition of ruthenium III chloride $RuCl_3 \cdot nH_2O$ in neutral atmosphere Ar is presented in Fig. 2 and its comparison with Fig. 1 suggests a close resemblance of hydrated $RuCl_3$ decomposition in inert and oxidative atmospheres. In Fig. 2 three stages of decomposition are also visible: first, three-step dehydration up to 400 °C, second, two step dechlorination–oxidation up to 800 °C and third one de-oxidation above 1000 °C. The exothermic DTA effect at 570 °C is assigned to crystallization process of amorphous fairly dehydrated ruthenium chloride $RuCl_3$. The temperature programmed sequence of events is confirmed by the MS profiles representing successively the evolution of H_2O, HCl, Cl_2 and finally O_2. The presence of oxygen in $RuCl_3$ sample may originate from a successive replacement reaction $Cl^- \rightarrow OH^- \rightarrow O^{2-}$ taking place during sample dechlorination–reoxidation process leading to RuO_x formation. The evolution of oxygen represents the last stage of sample decomposition above 1000 °C $RuO_x \rightarrow Ru^0 + (x/2)O_2$.

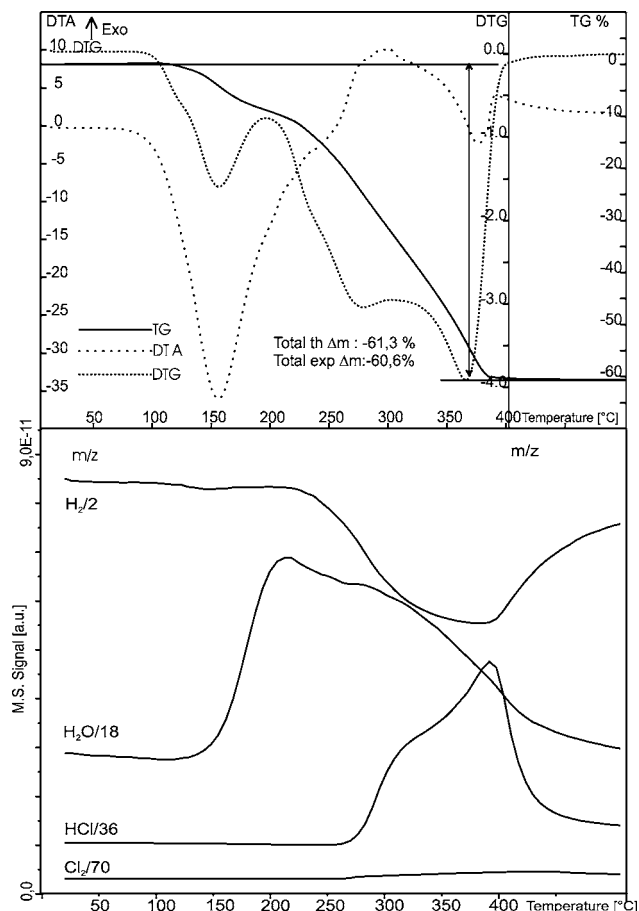The decomposition of ruthenium III chloride $RuCl_3 \cdot nH_2O$ in reductive atmosphere 2% H_2–98% Ar is presented in Fig. 3. The character of reductive decomposition of hydrated ruthenium chloride is completely different. Thermally induced sample reduction is accomplished up to 400 °C and the dehydration above 100 °C represented by MS profile of water ($m/z = 18$) is heavily overlapped with reduction of $RuCl_3$ taking place in temperature range 200–400 °C. The reduction of $RuCl_3$ seems to be represented by two-step reduction described by DTG curve and MS profiles for H_2 consumption ($m/z = 2$) and HCl evolution ($m/z = 36$). The total decrease in sample weight about 60% is in a good accordance with that obtained in oxidative atmosphere being about 62%.

3.2. Rhodium III chloride—RhCl₃·3H₂O

The decomposition of rhodium III chloride $RhCl_3 \cdot 3H_2O$ in oxidative atmosphere 2% O_2–98% Ar is presented in Fig. 4. The process starts at about 100 °C and the changes of TG and DTG curves are accompanied by DTA peaks: three endothermic (t_{min} about 170, 295 and 400) and one exothermic (t_{max} about 510), respectively. The corresponding effects of water evolution ($m/z = 18$) represents two-step sample dehydration
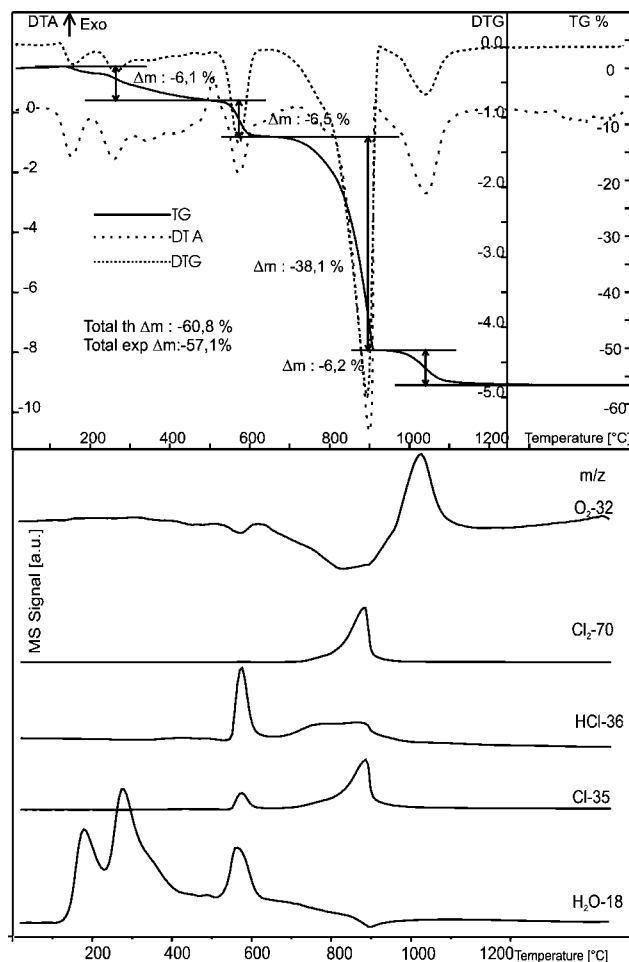
Fig. 4. Thermal decomposition of $RhCl_3 \cdot 3H_2O$ in oxidative atmosphere (2% O_2–98% Ar).

Fig. 5. Thermal decomposition of $RhCl_3 \cdot 3H_2O$ in inert atmosphere (Ar).

up to 500 °C followed by intermediate crystallization at about 500 °C (exothermic DTA effect) and completion of dehydration combined with the first stage of chloride phase decomposition (530–640 °C). Sample dechlorination-oxidation takes place in temperature range 530–930 °C as a two-step process, comprising Δm values 6.5 and 38.1%, respectively. The examination of MS profiles shows that the first stage of $RhCl_3$ decomposition involves dechlorination according to reaction $H_2O + Cl^- \rightarrow HCl + OH^-$ or $OH^- + Cl^- \rightarrow HCl + O^{2-}$, manifesting the evolution of HCl ($m/z = 36$), whereas the second stage is rather dominated by reaction $0.5O_2 + 2Cl^- \rightarrow Cl_2 + O^{2-}$. The simultaneous evolution of HCl and Cl_2 products ($m/z = 36$) and Cl_2 ($m/z = 70$) and the consumption of H_2O and O_2 reagents ($m/z = 18$ and $m/z = 32$) confirm the above pathways of dechlorination process. Both steps of dechlorination are accompanied by rather strong DTA endothermic peaks (t_{min} about 540, and 850). Above 900 °C sample de-oxidation takes place and this process is illustrated by TG, DTG changes ($\Delta m = 6.2\%$) and a strong endothermic DTA effect accompanied by MS oxygen evolution ($m/z = 32$). The total change of sample mass was about 56.9%. The following
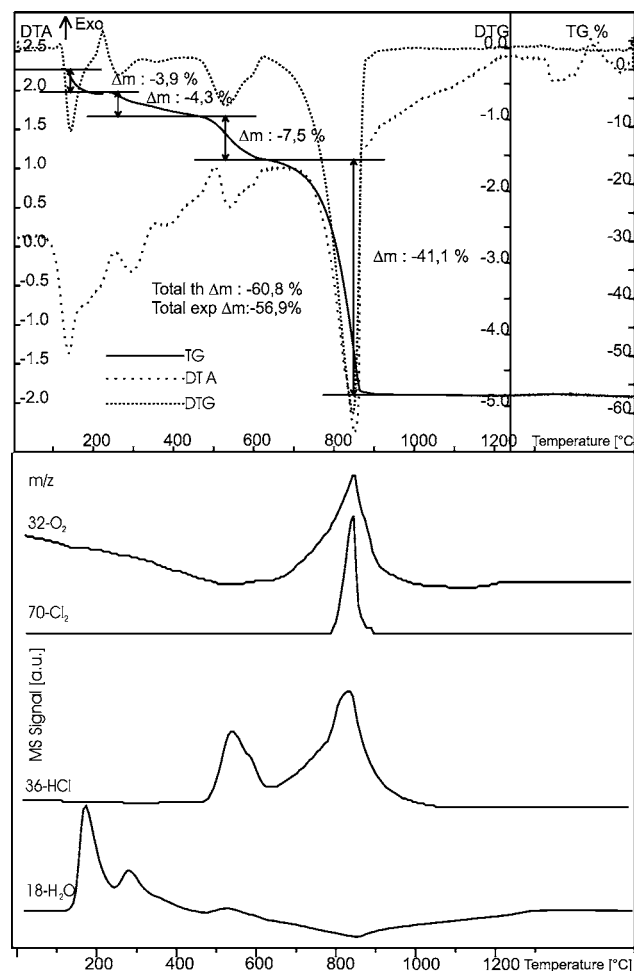
sequence of temperature programmed successive events of $RhCl_3 \cdot 3H_2O$ decomposition can be anticipated: dehydration, crystallization, dechlorination plus oxidation and final dissociation of ruthenium oxide resulting in metallic rhodium phase.

The decomposition of rhodium III chloride $RhCl_3 \cdot 3H_2O$ in neutral atmosphere Ar is presented in Fig. 5 and this process is very similar to decomposition described above, in oxidative atmosphere (Fig. 4). Instead of transformation $RhCl_3$ into Rh_2O_3 the lack of gaseous oxygen favours the direct decomposition according to reaction like $RhCl_2OH \rightarrow Rh^0 + HCl + 0.5Cl_2 + 0.5O_2$. This process is accomplished up to 900 °C and the total weight loss is practically the same ($\Delta m = 56.8\%$). On the basses of the data of Fig. 5 the sequence of temperature programmed events can be as follow: dehydration, crystallization and finally dechlorination leading directly to metallic rhodium phase Rh^0. The proposed mechanism is confirmed by the MS profiles representing successively the evolution of H_2O, HCl, Cl_2 and O_2. The presence of oxygen or hydroxyl group into $RuCl_3$ crystal phase may originate from replacement reaction $Cl^- + H_2O \rightarrow OH^- + HCl$ or
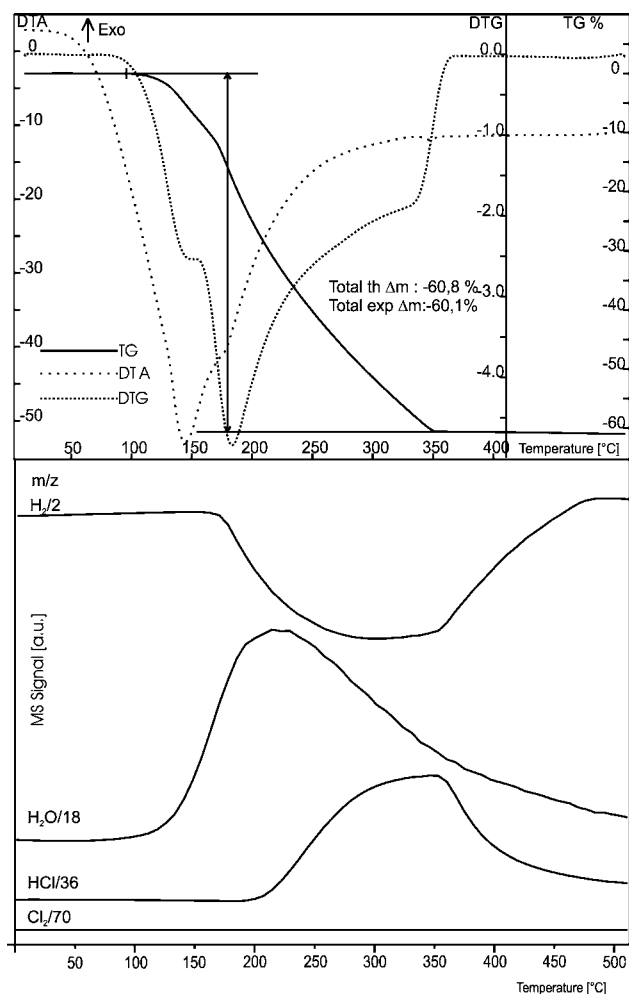
Fig. 6. Thermal decomposition of $RhCl_3 \cdot 3H_2O$ in reductive atmosphere (2% H_2–98% Ar).

Fig. 7. Thermal decomposition of $PdCl_2$ in oxidative atmosphere (2% O_2–98% Ar).

dehydration reaction $2OH^- \rightarrow O^{2-} + H_2O$ taking place during the first step of simultaneously occurring sample dechlorination–dehydration process [1].

The decomposition of rhodium III chloride $RhCl_3 \cdot 3H_2O$ in reductive atmosphere 2% H_2–98% Ar is presented in Fig. 6. As it was expected the character of reductive decomposition of hydrated rhodium chloride is completely different from that characteristic of decomposition in oxidative and neutral atmospheres (compare Figs. 4 and 5). Temperature programmed reduction of $RhCl_3$ is represented by MS profiles of H_2 consumption ($m/z = 2$) and HCl evolution ($m/z = 36$). The dehydration process starting above $100\,^\circ C$ and represented by MS profile of water ($m/z = 18$) is heavily overlapped with $RhCl_3$ reduction taking place in temperature range $200–400\,^\circ C$. The total loss of sample weight about 56.9% is in a good accordance with the stoichrometric value 60.8% calculated on the basis of equation $RhCl_3 \cdot 3H_2O + 1.5H_2 \rightarrow Rh + 3H_2O + 3HCl$. Close resemblance of reduction pathway for hydrated rhodium and ruthenium chlorides is rather undoubtful (compare Fig. 3).
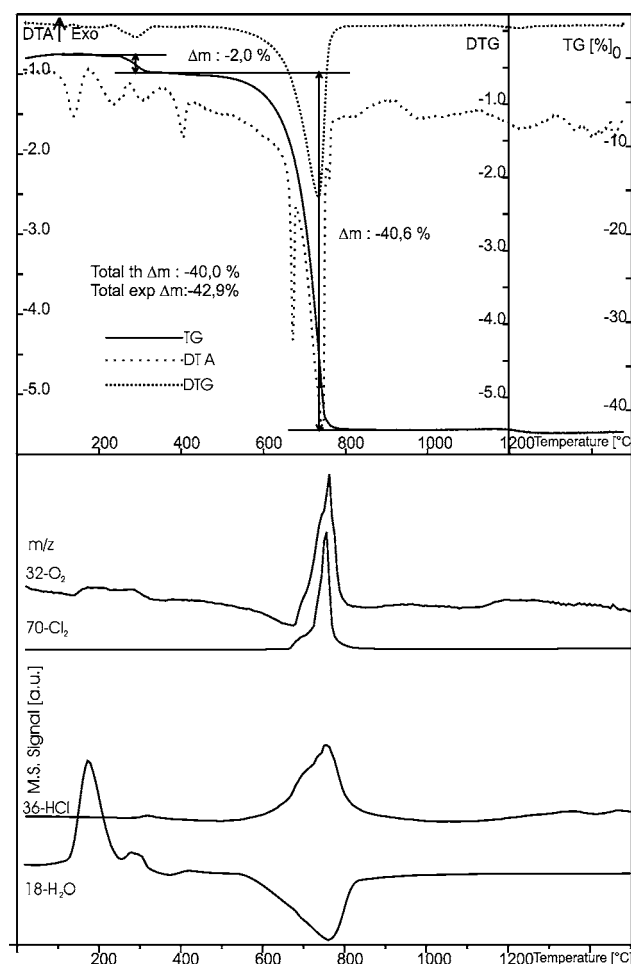
3.3. Palladium II chloride—$PdCl_2$

The decomposition of palladium II chloride $PdCl_2$ in oxidative atmosphere 2% O_2–98% Ar is presented in Fig. 7. The process of water removal taking place in the temperature range $100–300\,^\circ C$ and the changes of TG and DTG curves are accompanied by two endothermic DTA peaks: (t_{min} about 160 and $240\,^\circ C$). Although palladium II chloride supposedly was nominally water free but the investigated sample appeared to contain about 2% of water. Two narrow endothermic DTA peaks (t_{min} about 300 and $410\,^\circ C$) were attributed to crystal phase transformation of $PdCl_2$. The one stage of palladium chloride phase transformation into metallic palladium phase takes place in temperature range $600–800\,^\circ C$. Sample dechlorination results in weight loss Δm about 40.6%. The examination of MS profiles shows that transformation $PdCl_2 \rightarrow Pd^0$ involves water uptake from gaseous atmosphere and the evolution of O_2, HCl and relatively small amount of Cl_2. Such process can be described by general reaction $PdCl_2 + H_2O \rightarrow Pd^0 + HCl + 0.5O_2 + 0.5Cl_2$. The following sequence of temperature programmed decomposition of $PdCl_2 \cdot nH_2O$ can be anticipated: dehydration, crystal phase
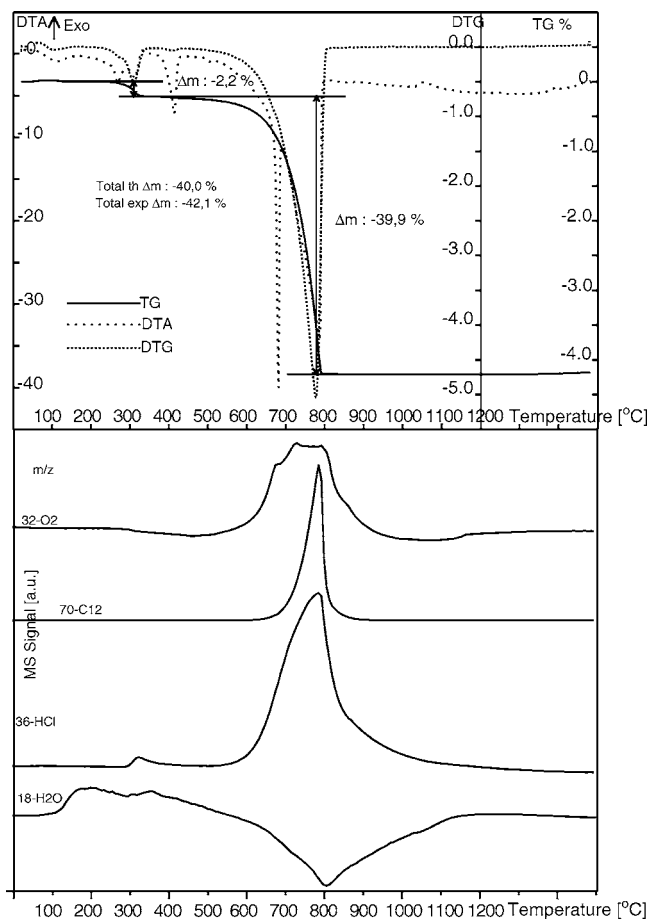
Fig. 8. Thermal decomposition of PdCl$_2$ in inert atmosphere (Ar).

Fig. 9. Thermal decomposition of PdCl$_2$ in reductive atmosphere (2% H$_2$–98% Ar).

transformation and finally dechlorination leading to metallic palladium phase.

The decomposition of palladium II chloride PdCl$_2$ in inert Ar atmosphere is presented in Fig. 8. The process of water removal taking place in the temperature range 100–300 °C and the changes of TG and DTG curves are accompanied by endothermic DTA peak: (t_{min} about 110 °C). Although palladium II chloride was to be water free but investigated sample appeared to contain about 2% of water. Two narrow endothermic DTA peaks (t_{min} about 305 and 410 °C) were attributed to crystal phase transformation of PdCl$_2$. The one stage of palladium chloride phase transformation into metallic palladium phase takes place in temperature range 600–800 °C. Sample dechlorination results in weight loss Δm about 39.9%. The examination of MS profiles shows the same kind of transformation as during PdCl$_2 \rightarrow$ Pd^0 decomposition in oxidative 2% O$_2$–98% Ar atmosphere (compare Figs. 7 and 8).

The reduction of palladium II chloride PdCl$_2$ in reductive atmosphere 2% H$_2$–98% Ar is presented in Fig. 9. Temperature programmed reduction starts at about 50 °C and is accomplished bellow 300 °C being represented by both TG, DTG, DTA curves and MS profiles for H$_2$ consumption ($m/z = 2$) and HCl evolution ($m/z = 36$). The dehydration process starting above 50 °C and represented by MS profile
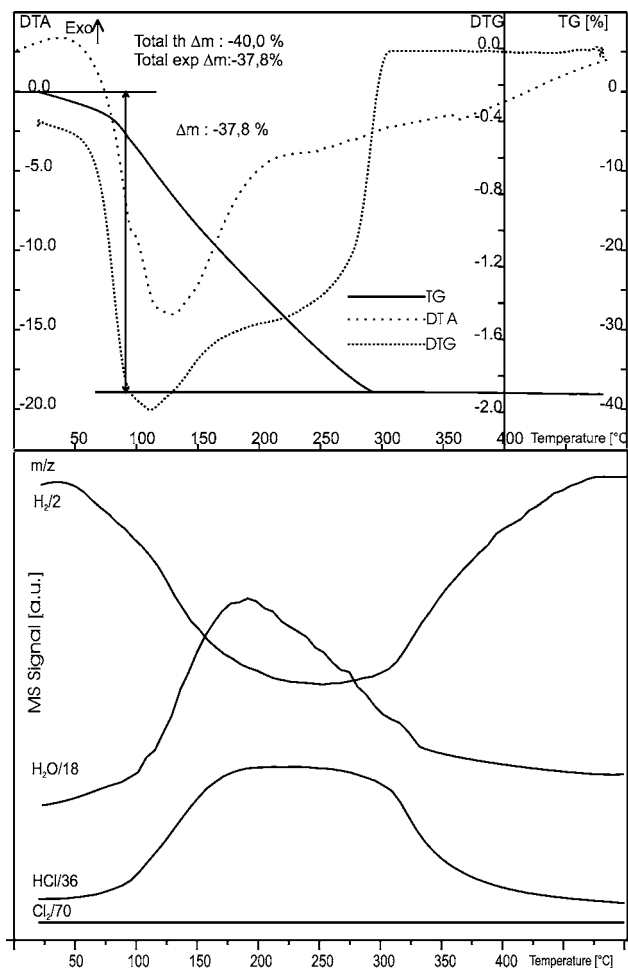
of water ($m/z = 18$) is heavily overlapped with PdCl$_2$ reduction. The total loss of sample weight was about 37.8% being in a good accordance with that stoichrometric value 40.0% calculated on the basis of equation PdCl$_2$ + H$_2$ → Pd + 2HCl. Again, a close resemblance of hydrogen reduction pathway for rhodium, ruthenium and palladium chlorides is un doubtful (compare Figs. 3, 6 and 9).

3.4. Iridium III chloride—IrCl$_3$·3H$_2$O

The decomposition of iridium III chloride IrCl$_3$·3H$_2$O in oxidative atmosphere 2% O$_2$–98% Ar is presented in Fig. 10. The entire process takes place up to 1200 °C and it can be divided into three not overlapped temperature regions: dehydration 50–400 °C, dechlorination–reoxidation 650–750 °C and dissociative deoxidation of iridium oxide—above 900 °C. The corresponding sample weight losses are presented in Fig. 10. The total mass decrease of sample was about 50.1%. The above assignment of IrCl$_3$·3H$_2$O decomposition was done on the changes of TG, DTG curves and DTA peaks and confirmed by MS profiles of gaseous products H$_2$O, HCl, O$_2$ and Cl$_2$. The additional
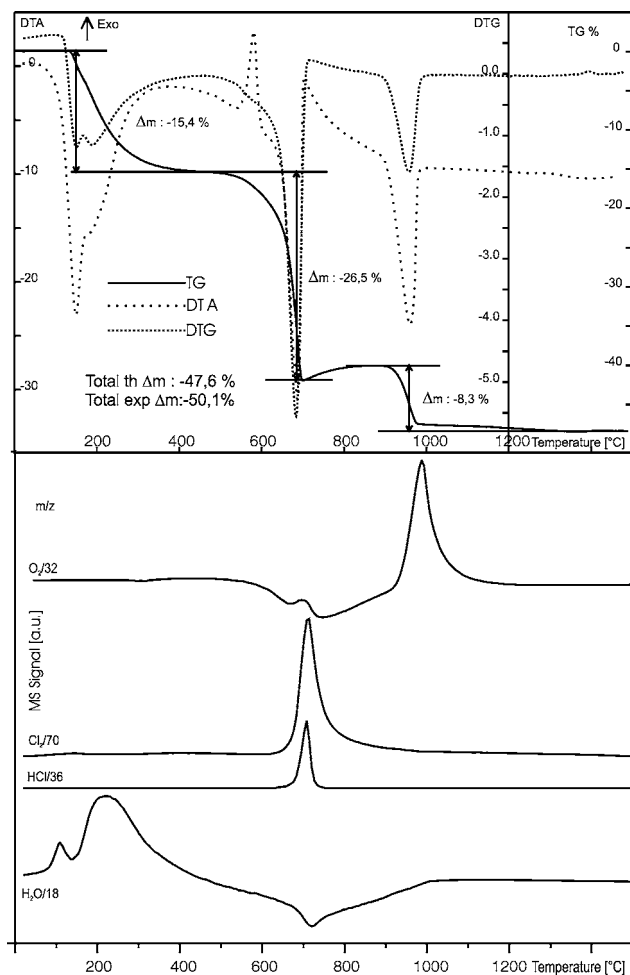
Fig. 10. Thermal decomposition of $IrCl_3 \cdot 3H_2O$ in oxidative atmosphere (2% O_2–98% Ar).

Fig. 11. Thermal decomposition of $IrCl_3 \cdot 3H_2O$ in inert atmosphere (Ar).

DTA exothermic effect (t_{max} about 590 °C) is assigned to crystallization process of amorphous $IrCl_3$ phase. This crystallic product undergoes further transformation according to general reaction $IrCl_3 + 1.5H_2O + 0.25O_2 \rightarrow IrO_2 + 3HCl$. In fact dechlorination–oxidation process $IrCl_3 + 1.5H_2O \rightarrow 1.5Ir_2O_3 + 3HCl$ taking place in temperature range 550–700 °C (TG decrease) is followed by an additional oxidation $1.5Ir_2O_3 + 0.5O_2 \rightarrow IrO_2$ in temperature range 700–800 °C (TG increase). Thus, oxygen in iridium oxide phase originates both from gaseous O_2 molecules and water or OH hydroxyl groups. Above 900 °C thermal dissociation takes place $IrO_2 \rightarrow Ir^0 + O_2$. Generally, the sequence of temperature programmed successive events of $IrCl_3 \cdot 3H_2O$ decomposition can be anticipated: dehydration, recrystallization, dechlorination plus oxidation and final dissociation of iridium oxide leading finally to metallic iridium phase.

The decomposition of iridium III chloride $IrCl_3 \cdot 3H_2O$ in inert Ar atmosphere is presented in Fig. 11. The process takes place up to 1000 °C and the only considerable differences result from the obvious lack of oxygen in gaseous atmosphere. The intermediate reaction
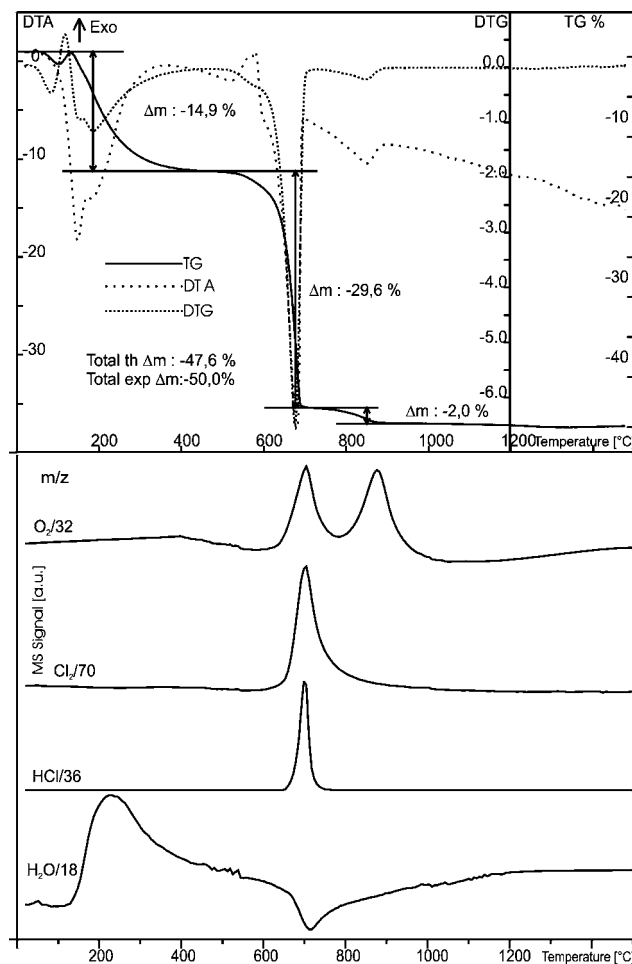
$IrCl_3 + H_2O \rightarrow IrCl_2OH + HCl$ seems to be responsible for the first replacement stage of subsequent sequence of events $Cl^- \rightarrow OH^- \rightarrow O^{2-} \rightarrow (1/2)O_2$ taking place in the first coordination sphere of iridium ion Ir^{3+}. Thus, the partial transformation of iridium chloride into none stoichrometric iridium oxide IrO_x results from the equation $Ir(OH)_xCl_{6-x} \rightarrow IrO_x + xHCl + (3-x)Cl_2$ describing the stoichrometry of octahedral coordination of iridium ion. The dissociative decomposition of IrO_x phase takes place at much lower temperature (about 100 °C) than in the oxidative atmosphere (compare Fig. 10). Total loss of sample weight was about 50% what is not only similar to the value obtained in oxidative atmosphere but also in accordance with the stoichrometry of following equation: $IrCl_3 \cdot 3H_2O \rightarrow Ir^0 + 3H_2O + (3/2)Cl_2$.

The process of iridium III chloride $IrCl_3 \cdot 3H_2O$ in reductive atmosphere 2% H_2–98% Ar is presented in Fig. 12. Once again it is very similar to the reduction profiles of described above ruthenium, rhodium and palladium chlorides (compare Figs. 3, 6 and 9). Temperature programmed reduction of $IrCl_3$ begins above 200 °C and is accomplished bellow 350 °C and is represented by MS profiles for H_2 consumption ($m/z = 2$) and HCl evolution ($m/z = 36$). The dehydration process
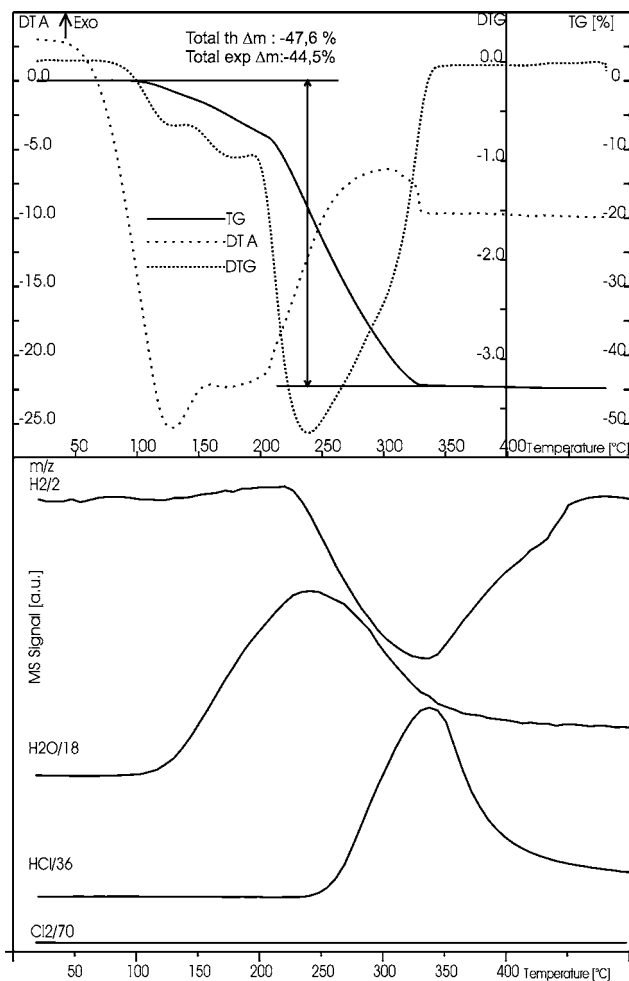
Fig. 12. Thermal decomposition of $IrCl_3 \cdot 3H_2O$ in reductive atmosphere (2% H_2–98% Ar).

Fig. 13. Thermal decomposition of $PtCl_4 \cdot 5H_2O$ in oxidative atmosphere (2% O_2–98% Ar).

starting above 100 °C and represented by MS profile of water ($m/z = 18$) is heavily overlapped with $IrCl_3$ reduction. The total loss of sample weight about 44.5% is in a good accordance with that stoichrometric value 46.1% calculated on the basis of equation $IrCl_3 \cdot 3H_2O + 1.5H_2 \rightarrow Ir^0 + 3H_2O + 3HCl$.

3.5. Platinum IV chloride—$PtCl_4 \cdot 5H_2O$

The decomposition of platinum IV chloride $PtCl_4 \cdot 5H_2O$ in oxidative atmosphere 2% O_2–98% Ar is presented in Fig. 13. The entire process takes place in temperature range 100–550 °C, much narrower than those found for described above ranges of decompositions of other noble metal chlorides. The process of complete decomposition $PtCl_4 \cdot 5H_2O \rightarrow Pt + 2Cl_2 + 5H_2O$ can be divided into three isolated temperature regions: dehydration process 100–300 °C and completely separated two stages of dechlorination-oxygenation and dechlorination-reduction processes 280–400 °C and 420–550 °C, respectively. The total decrease of sample mass was about 54.1%. The above assignment of $PtCl_4 \cdot 5H_2O$ decomposition was based on the changes of TG, DTG curves and DTA peaks and confirmed by

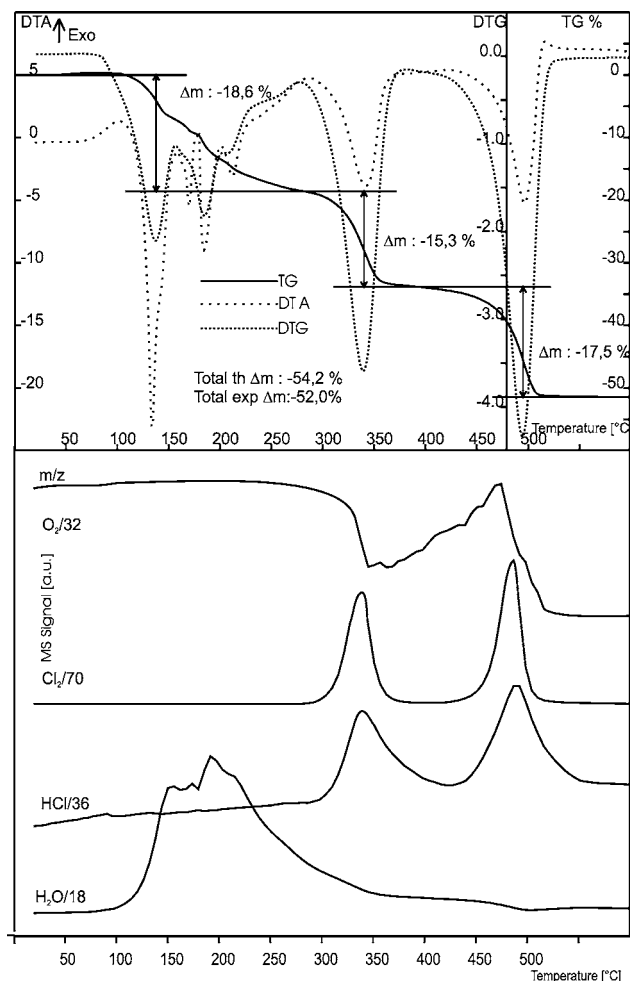MS profiles of gaseous products H_2O, HCl, O_2 and Cl_2. The successive stages can be described by following equations:

(1) four-step dehydration: $PtCl_4 \cdot 5H_2O \rightarrow PtCl_4 \cdot H_2O + 4H_2O$, $\Delta m = 18.6\%$;
(2) dechlorination: $PtCl_4 \cdot H_2O + (1/2)O_2 \rightarrow PtCl_2O_{1/2}(OH) + HCl + (1/2)Cl_2$, $\Delta m = 15.3\%$;
(3) dechlorination–reduction:
$PtCl_2O_{1/2}(OH) \rightarrow Pt^0 + HCl + (1/2)Cl_2 + (3/4)O_2$,
$\Delta m = 17.5\%$.

In fact, stage 2 is a partial replacement of chlorine ions by oxygen atom taken from the first coordination sphere of Pt^{4+} whereas final stage 3 leads to decomposition of Pt(IV) complex into metallic platinum and gaseous products: HCl, Cl_2 and O_2. The total decrease of sample mass is about 51.4% being the sum of the above Δm values and is in a good accordance with stoichrometry of $PtCl_4 \cdot 5H_2O$ complete decomposition $\Delta m_{th} = 54.2\%$.

The decomposition of platinum IV chloride $PtCl_4 \cdot 5H_2O$ in inert Ar is presented in Fig. 14 and it is very similar to that experiment carried out in oxidative atmosphere 2%
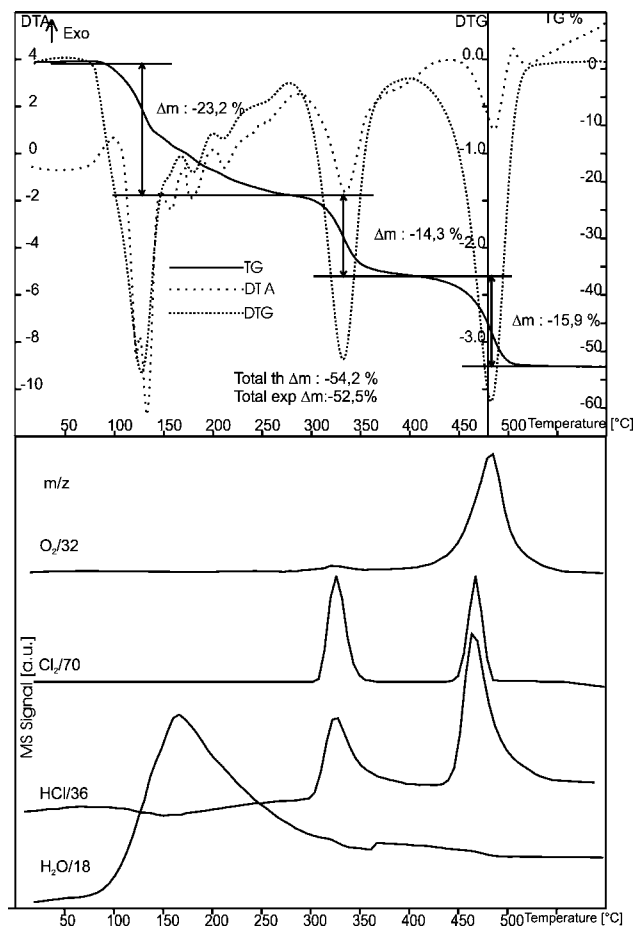
Fig. 14. Thermal decomposition of $PtCl_4 \cdot 5H_2O$ in inert atmosphere (Ar).

Fig. 15. Thermal decomposition of $PtCl_4 \cdot 5H_2O$ in reductive atmosphere (2% H_2–98% Ar).

O_2–98% Ar (compare Fig. 13). Once again, dehydration is four-step process and the accompanying mass loss Δm is about 18.6% The remarkable differences are limited to the source of origin for oxygen evolution in last stage of $PtCl_4 \cdot 5H_2O$ decomposition, taking into account the absence of oxygen in argon atmosphere and very small contribution of chlorine in gaseous products observed during both stages of platinum chloride dechlorination. The proposed explanation is supported on the larger involvement of water in the first stage of dechlorination. Thus, both water is the source of oxygen ligands in first coordination sphere of platinum ion Pt^{4+} and the same water molecule is responsible for HCl formation. The first stage of dechlorination should be modified in following way: $PtCl_4 + H_2O \rightarrow PtCl_2O + 2HCl$, $\Delta m = 15.3\%$ whereas the final stage of decomposition according to equation: $PtCl_2O + H_2O \rightarrow Pt^0 + 2HCl + O_2$, $\Delta m = 17.5\%$. Such approach also explains the presence of small amount of chlorine in gaseous products of platinum chloride decomposition in inert atmosphere. The total decrease of sample mass being the sum of the above Δm values and it is in a good accordance not only with the stoichrometry of $PtCl_4 \cdot 5H_2O$ complete decomposition $\Delta m_{th} = 54.2\%$ but also with value 51.4% obtained for oxidative atmosphere.
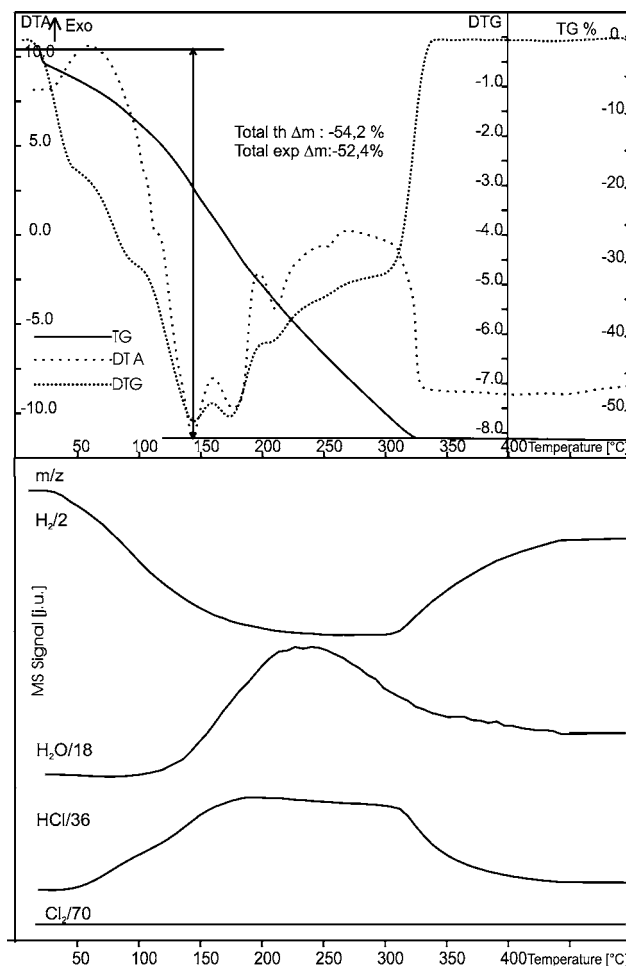
The process of platinum IV chloride $PtCl_4 \cdot 5H_2O$ in reductive atmosphere 2% H_2–98% Ar is presented in Fig. 15. Reduction behavior is very similar to the reduction profiles of described above ruthenium, rhodium, palladium and iridium hydrated chlorides (compare Figs. 3, 6, 9 and 12). Temperature programmed reduction of platinum IV chloride $PtCl_4 \cdot 5H_2O$ occurs between 50 and 350 °C and is represented by MS profiles for H_2 consumption ($m/z = 2$) and HCl evolution ($m/z = 36$). The dehydration process begins above 100 °C and takes place up to 350 °C being heavily overlapped with $PtCl_4$ reduction. The total loss of sample weight about 54.2% is in a good accordance with that stoichrometric value 52.4% calculated on the basis of equation $PtCl_4 \cdot 5H_2O + 2H_2 \rightarrow Pt + 2H_2O + 3HCl$.

4. Discussion

The comparative study of thermal behavior of the noble metal hydrated chlorides Ru, Rh, Pd, Ir and Pt in the wide temperature range, up to 1500 °C and in different atmospheres: oxidative, neutral and reductive has been presented.

The process of decomposition in oxygen appeared very similar to decomposition in inert atmosphere. In both cases thermal decomposition of noble metal hydrated chloride $Me^{x+}Cl_x \cdot nH_2O$ is characterized by several following intermediate processes:

1. Several-step successive dehydration $Me^{x+}Cl_x \cdot nH_2O \rightarrow Me^{x+}Cl_x \cdot pH_2O + (n-p)H_2O$ combined with the formation of amorphous metal chloride phase in temperature range from 100 up to about 500 °C.
2. Crystallization of amorphous $Me^{x+}Cl_x \cdot pH_2O$ taking place in temperature range 500–600 °C for Ru, Rh and Ir (exothermic peaks on DTA curve).
3. One-step for Pd and Ir or two-step for Ru and Rh decomposition of $Me^{x+}Cl_x \cdot pH_2O$ in temperature range 550–900 °C depending on the kind of noble metal. In oxygen atmosphere only metallic Pd and metal oxides: RuO_2, Rh_2O_3 and IrO_2 are formed.
4. Thermally induced dissociation of $MeO_{x/2}$ into Me metal and oxygen occurs above 950 °C for Rh_2O_3 and IrO_2 and above 1100 for RuO_2.

Generally, the mechanism of platinum IV chloride $PtCl_4 \cdot 5H_2O$ decomposition in oxidative O_2 or inert atmosphere is analogical to above findings. The only difference refers to much lower temperature range of $PtCl_4 \cdot 5H_2O$ decomposition 100–500 °C. In the case of palladium II chloride two additional endothermic effects were observed and those peaks were assigned to crystalline $PdCl_2$ phase transformations [10]. Finally, temperature dependent formation of metallic Pt and Pd and metal oxides: RuO_2, Rh_2O_3 and IrO_2 reflects increasing order of noble metal oxide thermal stability: $Pt < Pd < Ru < Rh < Ir$.

The differences between decomposition of hydrated noble metal chlorides $Me^{x+}Cl_x \cdot nH_2O$ in oxidative O_2 and inert Ar atmospheres result from different level of gaseous oxygen content. In oxygen-rich atmosphere the sequence of successive events in coordination sphere of noble metal ion is following: $Cl^- \rightarrow H_2O \rightarrow OH^- \rightarrow O^{2-} \rightarrow O_2$. Final oxygen ions may originate both from gaseous oxygen and water molecules or hydroxyl groups. The decomposition pathway can be different depending on both oxygen content and degree of compound dehydration in the system.

Assuming the octahedral coordination of hydrated noble metal chlorides the general pathway of $Me^{x+}Cl_x \cdot nH_2O$ decomposition in oxygen and argon atmospheres can be described by following reaction equations:

(1) dehydration: $Me^{x+}Cl_x \cdot nH_2O \rightarrow Me^{x+}Cl_x(H_2O)_{6-x} + (n+x-6)H_2O$;
(2) partial dechlorination in argon: $Me^{x+}Cl_x(H_2O)_{6-x} \rightarrow Me^{x+}Cl_y(OH)_{6-y} + (x-y)HCl$;
(3) partial dehlorination in oxygen: $Me^{x+}Cl_x(H_2O)_{6-x} + (z/4)O_2 \rightarrow Me^{x+}Cl_{x-z}O_{z/2}(OH)_{6-y} + (x-y)HCl + (z/2)Cl_2$;
(4) dissociation in argon: $Me^{x+}Cl_y(OH)_{6-y} \rightarrow Me^0 + (6-y)HCl + (y/3)Cl_2 + (3-y/2)O_2$;
(5) dechlorination–oxidation: $Me^{x+}Cl_{x-z}O_{z/2}(OH)_{6-y} + ((x-z)/2)O_2 \rightarrow Me^{x+}O_{x/2} + (6-y)HCl + ((x+y-z-6)/2)Cl_2$;
(6) thermal dissociation: $Me^{x+}O_{x/2} \rightarrow Me^0 + (x/4)O_2$.

The above mechanism ignores the possibility of the increase of oxidation number of metal atom in oxygen treatment of metal chlorides as it was observed during dechlorination-oxidation stage of $Ru^{3+}Cl_3 \rightarrow Ru^{4+}O_2$ and $Ir^{3+}Cl_3 \rightarrow Ir^{4+}O_2$ displacement transformations.

The approach based on the above stages of metal hydrated chlorides comprises the characteristic sequence of simple successive steps: $Cl^- (H_2O) \rightarrow OH^- \rightarrow O^{2-} \rightarrow O_2$ occurring in the first coordination sphere of Me^{x+} ion leading finally to metallic phase formation. The quantitative comparison of the experimental and theoretical data is presented in Table 2. The evaluation is based on simple three stage decomposition sequence consisting of following partial processes: dehydration, dechlorination–oxidation and final de-oxidation. An acceptable mutual accordance between experimental and theoretical date confirms the validity of postulated general mechanism of noble metal hydrated chlorides.

The hydrogen reduction of noble metals Ru, Rh, Pd, Ir and Pt hydrated chlorides can be described by two simultaneously occurring processes according to reaction equations:

Table 2
Theoretical and experimental weight loses for hydrated chlorides from 8 to 10 groups of Periodic System

Compound	Δm	Dehydration (%)	Dechlorination–oxidation (%)	Deoxydation (%)	Total (%)
$RuCl_3 \cdot 3H_2O$	Theoretical	20.6	28.5	12.2	61.3
	Experimental	20.7	28.0	12.9	61.6
$RhCl_3 \cdot 3H_2O$	Theoretical	20.4	31.3	9.1	60.8
	Experimental	12.6	38.1	6.2	56.9
$PdCl_2$	Theoretical	–	40.0	–	40.0
	Experimental	1.2	40.6	–	41.8
$PtCl_4 \cdot 5H_2O$	Theoretical	21.0	16.6, 16.6	–	54.2
	Experimental	18.6	15.3, 17.5	–	51.4
$IrCl_3 \cdot 3H_2O$	Theoretical	15.3	23.3	9.0	47.6
	Experimental	15.4	26.5	8.3	50.2

- dehydration: $Me^{x+}Cl_x \cdot nH_2O \rightarrow Me^{x+}Cl_x + nH_2O$;
- reduction: $Me^{x+}Cl_x + (x/2)H_2 \rightarrow Me^0 + xHCl$.

The hydrogen reduction of hydrated noble metal chlorides $Me^{x+}Cl_x \cdot nH_2O$ depends only slightly on the kind of metal. All hydrated chlorides are easily reducible in temperature range from 50–200 up to 300–400 °C depending on the kind of noble metal. Dehydration process is heavily overlapped with hydrogen reduction. Despite the obvious similarities the order of decreasing affinity of reduction in hydrogen is following: Pd > Pt > Rh > Ru > Ir.

5. Conclusion

Deeper insight into thermal decomposition of the noble metal hydrated chlorides Ru, Rh, Pd, Ir and Pt was achieved in their behavior in wide temperature range, up to 1500 °C and in different atmospheres: oxidative, neutral and reductive. General mechanism of the noble metal hydrated chlorides decomposition in oxygen and inert atmosphere has been postulated.

References

[1] I.S. Shaplygin, V.B. Lazarev, Thermal analysis, in: Proceedings of Fourth ICTA, Budapest, 1974, p. 1001.
[2] G. Bayer, H.G. Wiedemann, Thermal analysis, in: Proceedings of Fourth ICTA, Budapest, 1974, p. 1001.
[3] G. Bergeret, P. Gallezot, in: G. Ertl, H. Knözinger, J. Weitkamp (Eds.), Handbook of Heterogeneous Catalysis, vol. 2, VCH, Weinheim, 1997.
[4] G.J. Arteaga, J.A. Anderson, C.H. Rochester, J. Catal. 187 (1999) 219.
[5] A. Wiersma, M. van de Sand, H. den Hollander, van Bekkum, J. Catal. 177 (1998) 29.
[6] V.V. Pechkowskii, N.I. Worobiew, Zurnal Nieorganicheskoi Chemii 9 (1964) 12.
[7] S.E. Livingstone, The Chemistry of Ruthenium, Rhodium, Palladium, Osmium, Iridium and Platinum, Pergamon Texts in Inorganic Chemistry, vol. 25, Prergamon Press, 1973.
[8] S.I. Ginzburg, N.A. Ezewskaja, I.W. Prokofewa, N.W. Fedorenko, N.K. Belskii, Analiticheskaja chimija platinowych metalow, Nauka, Moscow, 1972.
[9] N.V. Sidgvick, The Chemical Elements and their Compounds, Clarendon Press, Oxford, 1950.
[10] D. Schultze, Termiczna analiza różnicowa, PWN, Warszawa, 1974.
[11] D. Roth, P. Gelin, M. Promet, E. Tena, Appl. Catal. A: Gen. 203 (2000) 37.
[12] B. Bachiller-Baeza, A. Guerrero-Ruiz, I. Rodriguez-Ramos, Appl. Catal. A: Gen. 192 (2000) 289.
[13] A. Babińska, F. Domka, Catal. Lett. 22 (1993) 327.